JOURNAL OF VIROLOGY, June 2006, p. 6072–6083 Vol. 80, No. 12
0022-538X/06/$08.00+0 doi:10.1128/JVI.02495-05

Dissociation of a MAVS/IPS-1/VISA/Cardif-IKKε Molecular Complex from the Mitochondrial Outer Membrane by Hepatitis C Virus NS3-4A Proteolytic Cleavage†

Rongtuan Lin,[1,3]* Judith Lacoste,[1] Peyman Nakhaei,[1,2] Qiang Sun,[1] Long Yang,[1,3] Suzanne Paz,[1,2] Peter Wilkinson,[1] Ilkka Julkunen,[4] Damien Vitour,[5] Eliane Meurs,[5] and John Hiscott[1,2,3]*

Terry Fox Molecular Oncology Group, Lady Davis Institute for Medical Research,[1] and Departments of Microbiology and Immunology[2] and Medicine,[3] McGill University, Montreal, Canada; National Public Health Institute and University of Helsinki, Helsinki, Finland[4]; and Department of Virology, Pasteur Institute, Paris, France[5]

Received 29 November 2005/Accepted 4 April 2006

Intracellular RNA virus infection is detected by the cytoplasmic RNA helicase RIG-I that plays an essential role in signaling to the host antiviral response. Recently, the adapter molecule that links RIG-I sensing of incoming viral RNA to downstream signaling and gene activation events was characterized by four different groups; MAVS/IPS-1-1/VISA/Cardif contains an amino-terminal CARD domain and a carboxyl-terminal mitochondrial transmembrane sequence that localizes to the mitochondrial membrane. Furthermore, the hepatitis C virus NS3-4A protease complex specifically targets MAVS/IPS-1/VISA/Cardif for cleavage as part of its immune evasion strategy. With a novel search program written in python, we also identified an uncharacterized protein, KIAA1271 (K1271), containing a single CARD-like domain at the N terminus and a Leu-Val-rich C terminus that is identical to that of MAVS/IPS-1/VISA/Cardif. Using a combination of biochemical analysis, subcellular fractionation, and confocal microscopy, we now demonstrate that NS3-4A cleavage of MAVS/IPS-1/VISA/Cardif/K1271 results in its dissociation from the mitochondrial membrane and disrupts signaling to the antiviral immune response. Furthermore, virus-induced IKKε kinase, but not TBK1, colocalized strongly with MAVS at the mitochondrial membrane, and the localization of both molecules was disrupted by NS3-4A expression. Mutation of the critical cysteine 508 to alanine was sufficient to maintain mitochondrial localization of MAVS/IPS-1/VISA/Cardif and IKKε in the presence of NS3-4A. These observations provide an outline of the mechanism by which hepatitis C virus evades the interferon antiviral response.

The hepatitis C virus (HCV) is an important cause of human chronic liver diseases (10, 21) and is a major public health problem. More than 170 million people worldwide are infected with HCV (38), a virus that is often associated with significant liver disease, including chronic active hepatitis, cirrhosis, and hepatocellular carcinoma (3). HCV is an enveloped virus classified in the *Flaviviridae* family (33). The positive-stranded viral RNA genome encodes a single polyprotein precursor that is processed into structural proteins (core, envelope protein 1, and envelope protein 2) and nonstructural proteins (p7, NS2, NS3, NS4A, NS4B, NS5A, and NS5B) by host and viral proteases (reviewed in references 32 and 39).

HCV and many viral infections are detected by the host cell through the presence of viral nucleic acids, such as single- and double-stranded RNA (dsRNA), triggering the production of interferons (IFN) and other cytokines that in turn stimulate innate and adaptive immune responses (16). Extracellular viral dsRNA is recognized by the Toll-like receptor 3 (TLR3) (1, 2), whereas intracellular viral dsRNA is detected by two recently characterized RNA helicases, RIG-I (41) and/or Mda5 (4, 18). The importance of the RIG-I pathway was confirmed with the generation of RIG-I-deficient mice (19), which revealed that RIG-I and not the TLR system played an essential role in the IFN antiviral response in most cell types, including fibroblastic, epithelial, and conventional dendritic cells. In contrast, plasmacytoid dendritic cells utilize TLR-mediated signaling in preference to RIG-I.

Upon dsRNA recognition and binding by its RNA helicase activity, RIG-I dimerizes and undergoes conformational alterations that enable the N-terminal CARD domain to interact with another downstream adapter protein(s). RIG-I signaling ultimately engages the IKK kinase complex and the stress-activated kinases, as well as the IKK-related kinases TBK1 and IKKε, leading to the phosphorylation and activation of NF-κB, ATF-2/c-jun, and interferon regulatory factor 3 (IRF-3) transcription factors (27). Coordinated activation of these factors results in the formation of a transcriptionally competent enhanceosome that triggers IFN-β production (30).

How HCV deals with the immediate host intracellular response to virus has been an area of intense study. Recent studies demonstrated that the HCV gene product NS3-4A protease complex, a multifunctional serine protease, efficiently blocked the RIG-I signaling pathway and contributed to virus persistence by enabling HCV to escape the IFN antiviral response. Nevertheless, RIG-I was not a direct target of NS3-4A, and likewise, the kinases TBK1 and IKKε were not subject to proteolytic cleavage by NS3-4A (8, 14, 37). Interestingly, the NS3-4A protease appears to target the TRIF/TICAM adapter of the TLR3 pathway and causes specific proteolytic cleavage

* Corresponding author. Mailing address: Lady Davis Institute for Medical Research, 3755 Cote Ste. Catherine, Montreal H3T 1E2, Quebec, Canada. Phone: (514) 340-8222, ext. 5272. Fax: (514) 340-7576. E-mail for Rongtuan Lin: rongtuan.lin@mcgill.ca. E-mail for John Hiscott: john.hiscott@mcgill.ca.

† Supplemental material for this article may be found at http://jvi.asm.org/.

of TRIF, although this pathway has a minimal role in triggering the IFN antiviral response (22a). Additional evidence for the importance of RIG-I comes from studies demonstrating that permissiveness for HCV RNA replication in Huh7.5 (6) cells is due to mutational inactivation of the RIG-I protein (37). Thus, RIG-I signaling appears to be an essential pathway regulating cellular permissiveness to HCV replication.

The adapter molecule that links RIG-I sensing of incoming viral RNA and downstream activation events was recently elucidated by four independent groups (20, 29, 35, 40). MAVS/IPS-1/VISA/Cardif contains an amino-terminal CARD domain and a carboxyl-terminal mitochondrial transmembrane sequence that localizes this protein to the mitochondrial membrane, thus suggesting a novel role for mitochondrial signaling in the cellular innate response (35). Under the name of Cardif, this protein was described by Meylan et al. to interact with RIG-I and recruits IKKα, IKKβ, and IKKε kinases through its C-terminal region. Importantly, Cardif was cleaved at its C-terminal end, adjacent to the mitochondrion-targeting domain, by the NS3-4A protease of hepatitis C virus (29). Li et al. subsequently demonstrated that NS3-4A cleavage of MAVS/IPS-1/VISA/Cardif resulted in its dissociation from the mitochondrial membrane and disruption of signaling to the antiviral immune response (23).

Using a combination of biochemical analysis, subcellular fractionation, and confocal microscopy, we demonstrate that the virus-inducible IKKε, but not TBK1, was strongly recruited to the mitochondria via MAVS/IPS-1/VISA/Cardif. Furthermore, stable expression of the NS3-4A complex in Huh8 HCV replicon cells or transient expression in Cos-7 cells disrupted the molecular complex between the MAVS/IPS-1/VISA/Cardif adapter and IKKε, resulting in relocation from the mitochondrial membrane to the cytosolic fraction and ablation of signaling to the antiviral immune response. These observations provide the outline of the mechanism for HCV evasion of the IFN signaling pathway.

MATERIALS AND METHODS

Plasmid constructions and mutagenesis. Plasmids encoding IKKε and TBK1, P2(2)-TK pGL3, IFNB/pGL3, IFNA14/pGL3, and pRLTK, have been described previously (25, 36). The cDNA encoding HCV NS3-4A was amplified from NS3-4A pcDNA3 plasmid (provided by M. Gale) and cloned into Flag pcDNA3.1/Zeo (Flag–NS3-4A). The cDNA encoding full-length human K1271 was amplified from a T-cell cDNA library and cloned into MYC pcDNA3.1/Zeo (Myc-KIAA1271) or Flag pcDNA3.1/Zeo (Flag-K1271). The point mutant A508 was generated by overlap PCR-mediated mutagenesis. The K1271 deletion mutants, including amino acids (aa) 1 to 508 [K1271(aa 1–150)], aa 1 to 467, aa 151 to 540, and aa 1 to 150 and a deletion of aa 150 to 467 (Δ150–467) and aa 150 to 502 (Δ150–502), were generated by PCR. DNA sequencing was performed for confirmation of mutations.

Cell culture, transfections, and luciferase assays. Human hepatoma Huh7 cells have been previously described (8). They were cultured in Dulbecco's modified Eagle's medium (DMEM) supplemented with 10% fetal bovine serum (FBS), 50 μg/ml gentamicin, and nonessential amino acids (1×). The same medium, also containing 500 μg/ml neomycin as a selection marker, was used to culture Huh8 cells, which are derived from Huh7 cells and stably express the HCV replicon. Human lung carcinoma A549 cells were cultured in F12K media supplemented with 10% FBS and 50 μg/ml gentamicin. Where indicated, A549 cells were infected with 10 multiplicities of infection of vesicular stomatitis virus (VSV) for 1 hour. Transfections for the luciferase assay were carried out in human embryonic kidney 293 (HEK293) cells grown in DMEM (GIBCO-BRL) supplemented with 10% fetal bovine serum, glutamine, and antibiotics. Subconfluent HEK293 cells were transfected by the calcium phosphate coprecipitation method with 100 ng of pRLTK reporter (*Renilla* luciferase for internal control), 100 ng of pGL-3 reporter (firefly luciferase, experimental reporter), 200 or 1,000 ng of ΔRIG-I, K1271, IKKε, or TBK1 expression plasmid, and 125, 500, or 2,000 ng of pcDNA3, Flag NS3-4A pcDNA3 zeo, or Flag A20 pcDNA3 zeo plasmid as indicated. The reporter plasmids were IFNB pGL3, ISRE-luc, P2(2)-TK pGL3, and IFNA14 pGL-3 reporter genes; the transfection procedures were previously described (24). At 24 h after transfection, reporter gene activity was measured by the Dual-Luciferase reporter assay, according to the manufacturer's instructions (Promega). Where indicated, cells were treated with Sendai virus (40 hemagglutinating units/ml) for the indicated time or 15 h for luciferase assays. Transfections for microscopy analyses were performed in African green monkey kidney cells (COS-7) cultured in DMEM containing 10% FBS and 50 μg/ml gentamicin. Briefly, cells were seeded on glass coverslips (12-mm diameter) and grown overnight to 50% confluence. At that point, cells were transfected with FuGENE 6 (Roche Diagnostics, Indianapolis, IN), using equal amounts (total of 0.4 μg DNA) of K1271-myc, IKKε-myc, and Flag–NS3-4A expression plasmids; as indicated, in the individual experiments, coverslips were harvested and processed for immunofluorescence staining 18 h later.

Generation of NS3-4A-expressing cell lines. Plasmids pcDNA3 zeo and Flag–NS3-4A pcDNA3 zeo were introduced into HEK293T cells by the calcium phosphate method. Cells were selected beginning at 48 h for approximately 3 weeks in DMEM containing 10% heat-inactivated calf serum, glutamine, antibiotics, and 100 μg/ml zeocin (Invitrogen).

Antibodies. K1271(aa 1–150) was expressed in *Escherichia coli* as a glutathione *S*-transferase fusion protein and purified by glutathione-Sepharose column chromatography. The recombinant proteins were injected into rabbits or guinea pigs to produce antisera against KIAA1271(aa 1–150). Similarly GST-K1271(aa 157–540) fusion proteins were injected into rabbits to produce antisera against KIAA1271(aa 157–540). Mouse anti-IKKε antibody was obtained from BD BioSciences (Mountain View, CA). Rabbit anti-TBK1 antibody was obtained from Upstate Biotech Inc. (Lake Placid, NY). The green (donkey anti-rabbit or anti-mouse immunoglobin [Ig] conjugated with AlexaFluor 488) and the red (donkey anti-guinea pig Ig conjugated with AlexaFluor 546) fluorochromes were obtained from Invitrogen/Molecular Probes.

Coimmunoprecipitation and Western blot analysis. Transient transfection, coimmunoprecipitation, and Western blot analysis were performed as previous described (26). In some experiments, mitochondria were isolated using the reagents and protocols of the mitochondria isolation kit (Pierce, Brockville, Canada).

Immunofluorescence staining and confocal microscopy. Cells were seeded on glass coverslips and grown overnight to 50% confluence. Staining of mitochondria was achieved by placing the cells in 25 nM MitoTracker Orange CMTMRos (MTO; Invitrogen/Molecular Probes, Eugene, OR), a red fluorochrome, for 30 min in a CO_2 incubator. Excess MTO was removed by further culturing the cells in fresh media for another 30 min. Coverslips were washed twice in warm culture media, fixed (37°C for 15 min) in a warm buffered fixation solution (3.7% paraformaldehyde and 10% FBS in phosphate-buffered saline [PBS]), and washed three times in PBS. Further steps were carried out at room temperature. Cells were permeabilized for 30 min in PBS containing 0.2% Triton X-100 and 3% IgG-free bovine serum albumin (BSA; Jackson ImmunoResearch, West Grove, PA). From this point on, all steps were done in PBS containing 0.5% IgG-free BSA. Coverslips were washed twice before being exposed to the primary antibodies for 60 min. Anti-K1271 antibody was diluted at 1:200, anti-IKKε antibody was used at 1 μg/ml, and anti-TBK1 antibody was diluted at 1:500. The primary antibody was washed off twice, before the coverslips were in the presence of fluorochromes (2 μg/ml, red and/or green, as indicated) for 60 min. Finally, coverslips were washed twice in BSA-PBS, washed once in water, and mounted on slides using ImmuMount (Thermo Electron Corporation, Pittsburgh, PA). Samples were analyzed on an inverted Axiovert 200 M Zeiss microscope equipped with an LSM 5-Pa confocal imaging system (Carl Zeiss Canada, Montreal, Quebec, Canada). Confocal images (0.3- to 0.5-μm slices) were acquired with a Plan-Apochromat ×63 oil objective, using the argon and HeNe laser lines (488 nm and 543 nm, respectively).

RESULTS

K1271 activates NF-κB and IRF-3/IRF-7 to induce interferon antiviral response. The observations that RIG-I, TBK1, and IKKε are not proteolytic substrates of NS3-4A indicated that an unidentified adapter(s) between RIG-I and the kinases may be a target for NS3-4A cleavage (8, 14). To this end, *mda-5* and RIG-I protein sequences were separated into do-

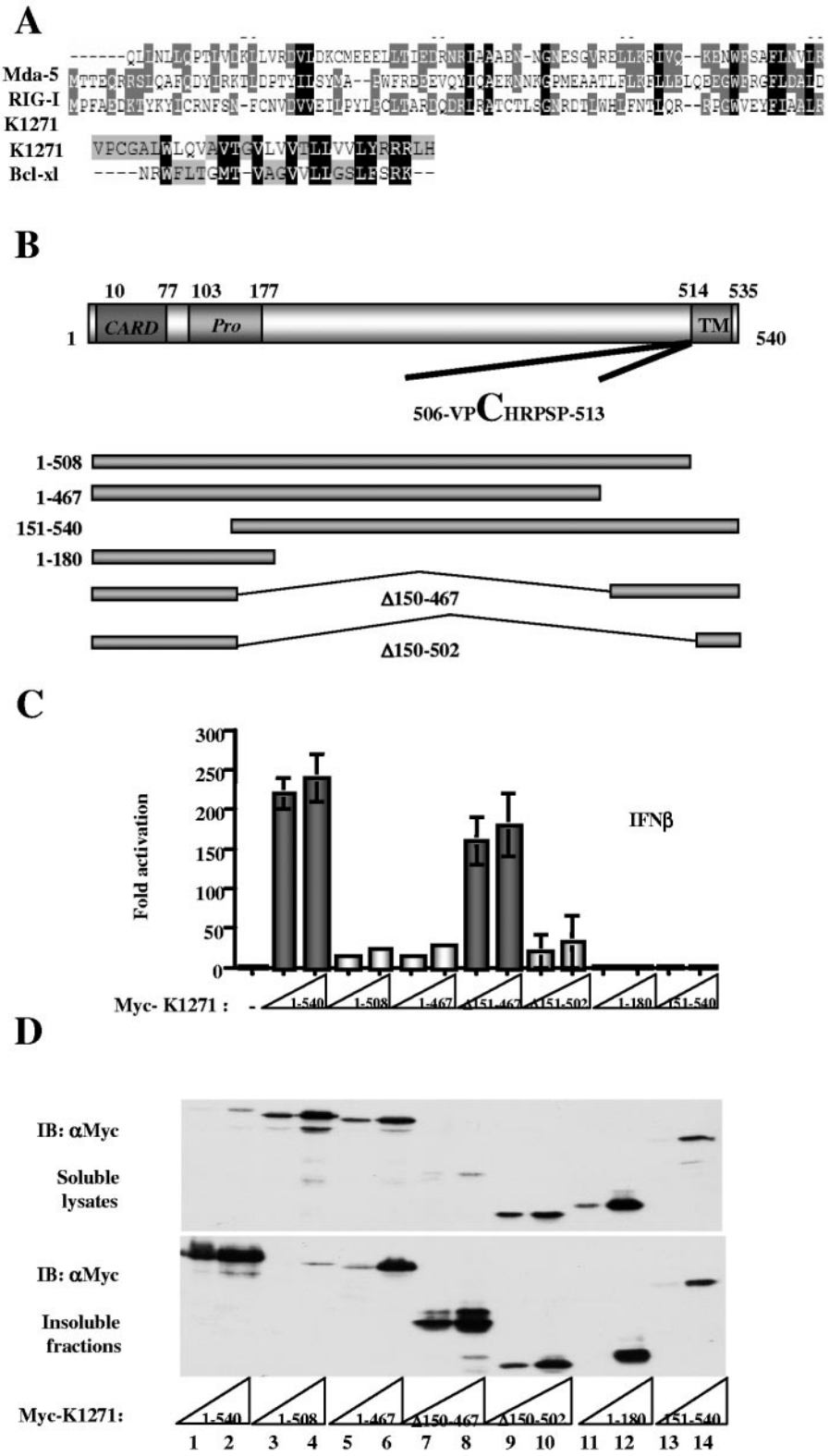

FIG. 1. Characterization of the RIG-I adapter. (A) Alignment of the CARD domains of Mda-5, RIG-I, and K1271. A BLAST alignment reveals CARD domain homology among the N-terminal sequences of RIG-I, Mda-5, and K1271. C-terminal alignment of the Leu-Val-rich region of K1271 and Bcl-xL is also shown. (B) Schematic representation of K1271. The 540-aa MAVS/IPS-1/VISA/Cardif molecule is shown schematically. The location of the CARD domain-containing, proline-rich region that interacts with TRAF6 and the C-terminal mitochondrial membrane region (TM) is shown. Also illustrated is the region adjacent to the TM containing cysteine 508, the target residues for the HCV NS3-4A protease. The different N- and C-terminal deletions used in this study are shown below the schematic. (C) N- and C-terminal

mains, and the domains were analyzed separately, creating a regular expression that represents the patterns of the domain. Next, a search program was written in python language (http://www.biopython.org); a database search was performed that identified an uncharacterized protein, KIAA1271(K1271), containing a single CARD-like domain at the N terminus and a Leu-Val-rich C terminus (Fig. 1A). Interestingly, analysis of the C terminus of K1271 revealed high homology with the C terminus of the antiapoptotic protein Bcl-xl. Following PCR amplification and subcloning, a series of K1271 deletion constructs were generated and tested for the capacity to stimulate the IFN-β promoter (Fig. 1B). Coexpression of K1271 strongly activated the IFN-β-dependent promoter and appeared to be the adapter linking RIG-I sensing to downstream signaling events. Both the N and C termini were essential for transactivation function, since deletion of either end of the protein eliminated transactivation (Fig. 1C). Interestingly, an expression construct that contained the N- and C-terminal domains but lacked the region between aa 150 and aa 467 also stimulated the IFN-β promoter (Fig. 1C), whereas a similar internal deletion construct removing the region between aa 150 and aa 502 was inactive, indicating that the region of K1271 between aa 467 and aa 502 was important for transactivation function. A direct correlation between downstream activation of the IFN-β promoter and subcellular localization was observed when the different K1271 deletion constructs were evaluated; wtK1271 and the active internal deletion Δ150–467 were localized to the insoluble fraction of cytoplasmic extracts (Fig. 1D, lanes 1, 2, 7 and 8), whereas the C-terminal truncation of aa 1 to 508 was localized exclusively in the soluble cytoplasmic extract (Fig. 1D, lanes 3 and 4). Other constructs, including the inactive internal deletion Δ150–502 and the deletions of aa 1 to 467, aa 1 to 180, and aa 151 to 540, redistributed to both the soluble and insoluble cytoplasmic fractions (Fig. 1D, lanes 5, 6, and 9 to 14).

Four independent groups reported that the same protein, alternately named MAVS/VISA/IPS-1-1/Cardif, acted downstream of RIG-I and stimulated the expression of IFN-β through the activation of NF-κB and IRF-3 (20, 29, 35, 40). The C-terminal Leu-Val domain was recognized as a mitochondrial transmembrane domain, and localization to the mitochondrial outer membrane was required for its function (35). Thus, MAVS/VISA/IPS-1-1/Cardif/K1271 is a critical adapter of the RIG-I pathway that links the "sensing" of incoming viral particles by RIG-I with downstream TBK1/IKKε kinases.

K1271 is a direct target of HCV protease NS3-4A. As shown by Meylan et al. (29), K1271 is a direct target of the HCV protease NS3-4A, with cleavage occurring adjacent to the transmembrane domain at Cys508. Increasing levels of coexpression of NS3-4A dramatically blocked K1271-driven gene expression from the IFN-β promoter (Fig. 2A), whereas the protease-inactive form of NS3-4A did not affect K1271-driven reporter gene expression. Concomitant with the inhibition of IFN-β-dependent gene expression, the size of K1271 was reduced and the amount of K1271 in the insoluble fraction of

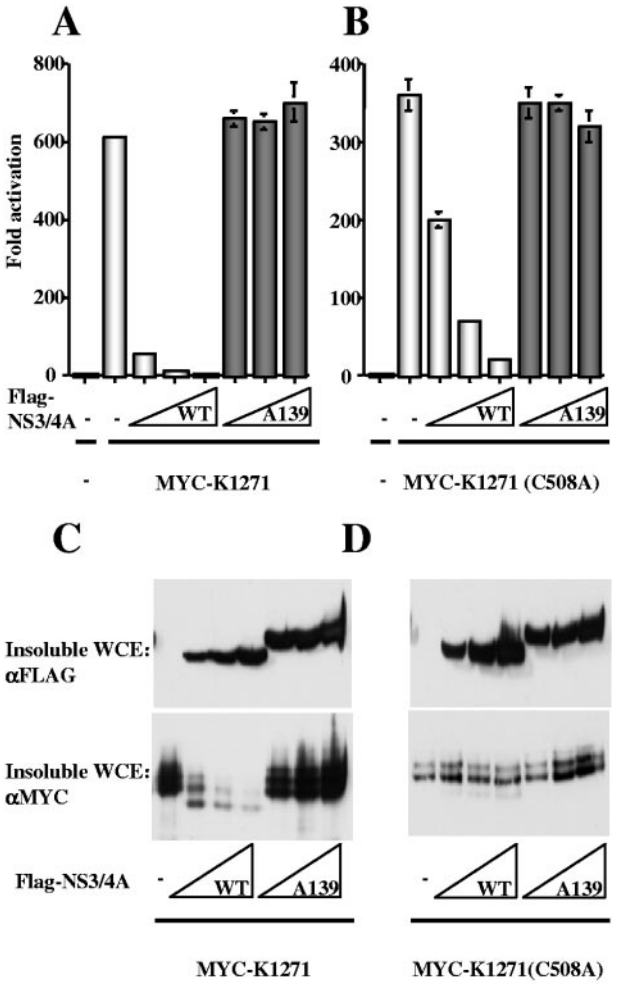

FIG. 2. Cleavage of K1271 and inhibition of K1271-mediated transactivation by NS3-4A. (A) HEK293 cells were transfected with 100 ng of pRLTK control plasmid, 100 ng of IFN-β–pGL3 reporter plasmid, and 200 ng of K1271 (A) or K1271(A508) (B) Myc-tagged expression plasmid, together with increasing amounts (250 ng, 500 ng, and 1,000 ng) of protease-active NS3-4A or inactive NS3-4A(A139) Flag-tagged expression plasmid as indicated. Luciferase activity was analyzed at 24 h posttransfection. (C and D) The soluble lysates and insoluble fractions were prepared from HEK293 cells used for panels A and B, equilibrated to the same volumes by sodium dodecyl sulfate-polyacrylamide gel electrophoresis loading buffer, and analyzed by immunoblotting with anti-Flag antibody M2 and anti-Myc antibody 9E10.

domains of K1271 are required for IFN-β promoter activation. HEK293 cells were transfected with 100 ng of pRLTK control plasmid and 100 ng of IFN-β–pGL3 reporter plasmid, with increasing amounts (200 ng and 1,000 ng) of different truncated forms of Myc-K1271 expression constructs as indicated. Luciferase activity was analyzed at 24 h posttransfection by the Dual-Luciferase reporter assay as described by the manufacturer (Promega). Relative luciferase activity was measured as activation (*n*-fold; relative to the basal level of reporter gene in the presence of pcDNA3 vector after normalization with cotransfected renilla luciferase activity); values are means ± standard deviations from three experiments. (D) Localization of active forms of K1271 to the insoluble fraction of the cytoplasm. The soluble lysates and insoluble fractions were prepared from the HEK293 cells used for panel C, equilibrated to the same volumes by sodium dodecyl sulfate-polyacrylamide gel electrophoresis loading buffer, and analyzed by immunoblotting with anti-Myc antibody 9E10.

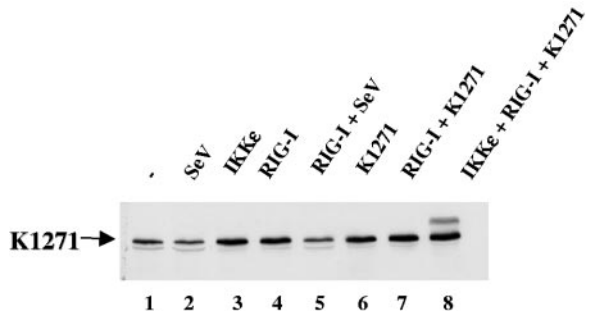

FIG. 3. Localization of K1271 to the mitochondria. HEK293 cells were transfected with combinations of 200 ng of IKKε and RIG-I; in some cases, cells were also infected with Sendai virus (40 hemagglutinating units/ml) at 24 h posttransfection for a total of 12 h. Mitochondrial extracts were prepared, and 50 μg of extract was run on 7.5% sodium dodecyl sulfate-polyacrylamide gel electrophoresis and immunoblotted with anti-K1271 antibody.

cytoplasmic extracts was decreased (Fig. 2C), whereas expression of the protease-inactive point mutant A139 did not alter the mobility or the amount of K1271. In contrast, the K1271 (C508A) point mutation remained localized in the insoluble cytoplasmic fraction, thus illustrating that K1271(C508A) was not cleaved by NS3-4A (Fig. 2D). However, K1271(C508A) IFN-β-driven gene activity was still decreased when NS3-4A was expressed, although with about 10-fold decreased efficiency, suggesting that NS3-4A may also target an undefined protein downstream of K1271.

The RIG-I RNA sensing molecule is highly inducible in response to virus, IFN, or retinoic acid treatment. To examine the inducibility and localization of K1271, a new rabbit polyclonal K1271 specific antibody was generated; detection of K1271 revealed that the adapter localized exclusively to the mitochondrial fraction. Furthermore, expression of K1271 was constitutive and expression of other components of the RIG-I pathway, including IKKε and RIG-I itself, or Sendai virus infection did not significantly alter the expression or mitochondrial localization of K1271 (Fig. 3).

Disruption of the mitochondrial localization of K1271 by NS3-4A. To examine the cleavage and mitochondrial localization of K1271 in human hepatoma cells, expression of K1271 was evaluated in both human hepatoma Huh7 and the HCV replicon-expressing Huh8 cells (5). As shown in Fig. 4A, full-length K1271 was detected in extracts of Huh7 cells, whereas the predominant form of K1271 in Huh8 cells was truncated. To further delineate the localization of K1271, mitochondrial extracts were prepared from HEK293 cells coexpressing NS3-4A (Fig. 4B). K1271 was easily detected in the mitochondrial but not cytosolic fraction of HEK293 cells (Fig. 4B, lanes 1 and 3), whereas in mitochondrial extracts from cells expressing NS3-4A, K1271 was not detected but rather was observed in the cytosol (Fig. 4B, lanes 2 and 4). Similar results were obtained when mitochondrial extracts were prepared from Huh7 and Huh8 cells; K1271 was detected in the mitochondria of Huh7 cells (Fig. 4B, lane 5), whereas in the NS3-4A-expressing HCV replicon cells, K1271 was detected almost exclusively in the cytosolic fraction (Fig. 4B, lane 8). Curiously, cytochrome *c* was not a good marker for mitochondrial isolation, since in the presence of NS3-4A, cytochrome *c*, but not mitochondrial hsp70, levels were reduced by NS3-4A expression (Fig. 4B, lanes 1, 2, 5, and 6).

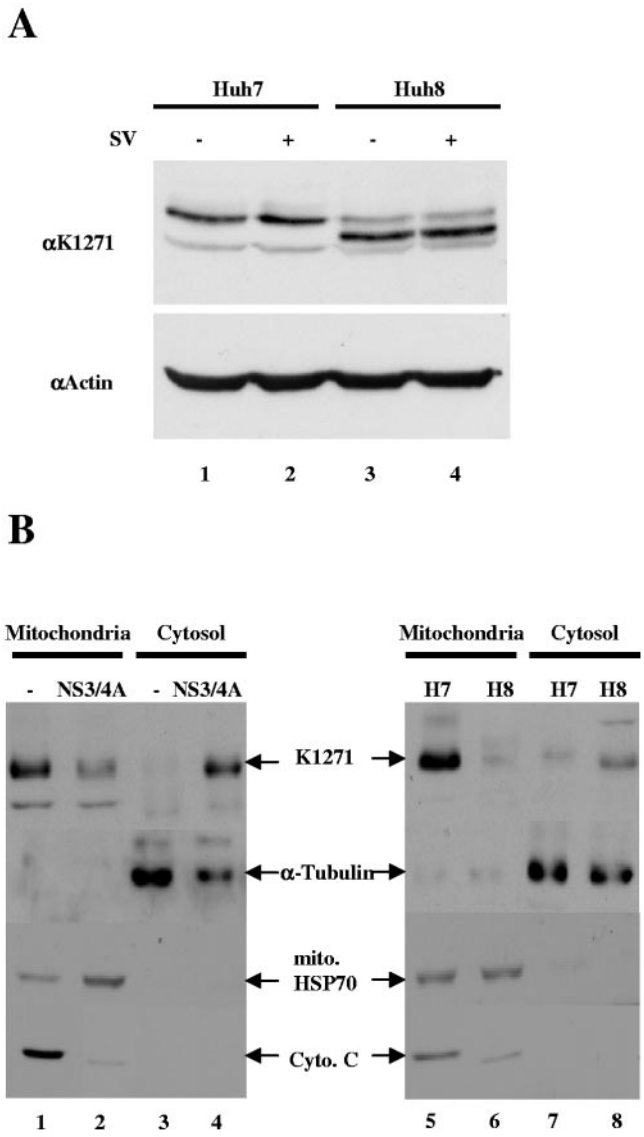

FIG. 4. Endogenous K1271 is cleaved in Huh8 HCV replicon cells. (A) Whole-cell extracts (50 μg) prepared from uninfected or Sendai virus-infected Huh7 or Huh8 cells were subjected to sodium dodecyl sulfate-polyacrylamide gel electrophoresis (SDS-PAGE) and probed with anti-K1271 and antiactin antibodies. (B) Mitochondrial and cytosolic fractions (50 μg) from HEK293T cells transfected with 200 ng of NS3-4A expression plasmid (lanes 1 to 4) were subjected to SDS-PAGE and analyzed by immunoblotting with anti-K1271, antitubulin, anti-cytochrome *c*, and anti-hsp70. Mitochondrial and cytosolic fractions (50 μg) from Huh7 (H7) and Huh8 (H8) cells (lanes 5 to 8) were also subjected to SDS-PAGE and analyzed by immunoblotting with anti-K1271, antitubulin, anti-hsp70, and anti-cytochrome *c*.

Confocal microscopy was also used to visualize the localization of K1271 in Huh7 cells (Fig. 5A to C) and in Huh8 cells (Fig. 5D to F). K1271 staining was localized predominantly to perinuclear bodies (Fig. 5A) that were costained with the mitochondrial marker MTO (Fig. 5B); merging of the signals demonstrated a strong colocalization of K1271 and mitochon-

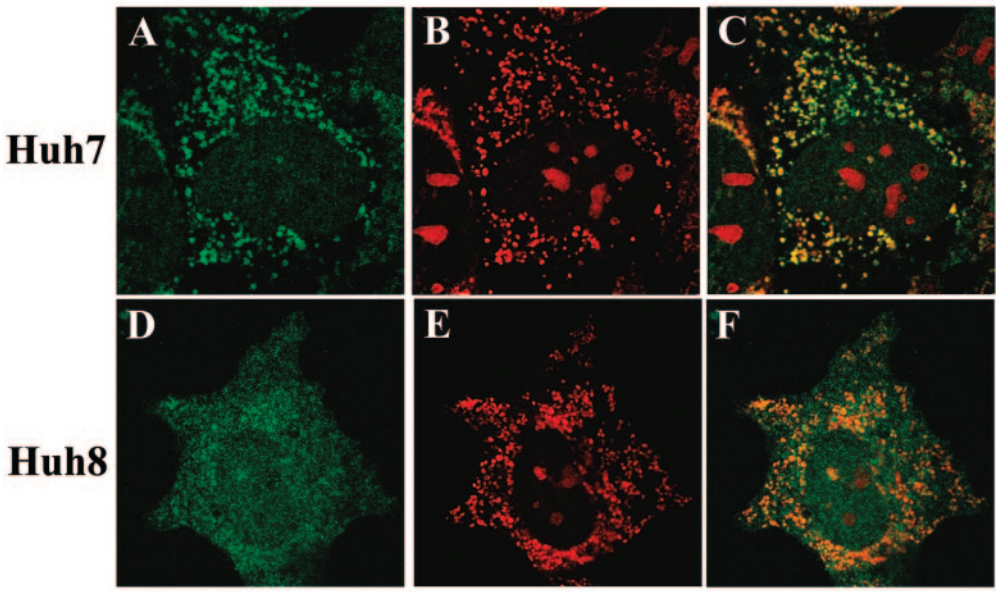

FIG. 5. Endogenous K1271 is cleaved in Huh8 HCV replicon cells. Huh7 (A to C) and Huh8 (D to F) cells were treated with MTO (B and E), fixed in paraformaldehyde, and stained for K1271 (A and D). Confocal fluorescent images were merged (C and F). K1271 was detected using rabbit anti-K1271 C-term and anti-rabbit AF488 antibodies.

dria (Fig. 5C). In contrast, staining of K1271 in NS3-4A-expressing Huh8 cells revealed a diffuse staining pattern (Fig. 5D) that did not reflect the pattern of mitochondrial staining (Fig. 5E). Merging of the fluorescence signals demonstrated that the localization of K1271 and mitochondria was no longer coincidental (Fig. 5F). Altogether, these results demonstrate that NS3-4A expression results in the cleavage of K1271 and the disruption of its localization to the mitochondrial membrane.

Distinct subcellular localizations of TBK1 and IKKε: recruitment of IKKε to K1271 localized at the mitochondrial membrane. To determine whether localization and/or recruitment of the virus-activated kinases TBK1 and IKKε could be observed in association with mitochondrion-localized K1271, endogenous K1271 and IKKε were visualized by confocal microscopy in lung epithelial A549 cells (Fig. 6). In control cells, IKKε was difficult to visualize due to its low level of expression, although K1271 was readily detected (Fig. 6, upper panels); however, in cells that were infected with VSV for 1 h, perinuclear IKKε was detected that colocalized with K1271 (Fig. 6, lower panels). The merging of the respective signals illustrated a strong colocalization of the two proteins. Interestingly, VSV-induced IKKε localized almost exclusively with mitochondria (detected by MTO) in the reticulotubular mitochondrial network (Fig. 7, upper panels), whereas no similar colocalization was observed between TBK1 and mitochondria (Fig. 7, lower panels). In fact, preliminary data suggest that TBK1 is partially associated with the early endosome marker EEA1, indicating an endosomal association of TBK1. Furthermore, the intensity and/or localization of TBK1 does not change with time after VSV infection (data not shown). Together, these data indicate distinct cytoplasmic localizations of IKKε and TBK1: the virus inducible IKKε is recruited to the mitochondrial network in association with K1271, while the constitutively expressed TBK1 localizes to a distinct cytoplasmic compartment.

Cleavage of the K1271-IKKε complex from the mitochondria by NS3-4A. To address the fate of the K1271-IKKε complex in the presence of the NS3-4A protease, transient expression studies of primate Cos-7 cells were undertaken (Fig. 8). As observed for the endogenous molecules shown in Fig. 6, costaining of transfected K1271 and IKKε revealed a strong colocalization in a typical mitochondrial pattern (Fig. 8, upper panels). Importantly, NS3-4A protease coexpression was sufficient to disrupt the mitochondrial localization of K1271-IKKε (Fig. 8, lower panels), resulting in a diffuse cytoplasmic staining pattern. When K1271 (C508A) was used in similar experiments, K1271-IKKε remained associated with the mitochondrial membrane (see Fig. S1 in the supplemental material). Similarly, a protease-inactive form of NS3-4A was unable to cleave the K1271-IKKε molecular complex from the mitochondrial surface (data not shown).

Inhibition of downstream IFN activation. The effects of NS3-4A on downstream gene activation events were next evaluated. As demonstrated in Fig. 2, coexpression of increasing amounts of NS3-4A strongly inhibited K1271-mediated activation of the IFN-β promoter (Fig. 9A), whereas a truncated form of K1271 [K1271(aa 1-508)] was unable to stimulate the IFN-β promoter and was also not inhibited by NS3-4A coexpression. A mutated form of K1271, K1271(C508A), with an alanine substitution at aa 508 which altered the site of NS3-4A cleavage was completely resistant to cleavage (Fig. 2). However, coexpression of the NS3-4A complex still inhibited K1271(C508A)-mediated transactivation more than 10-fold (Fig. 9A).

To verify whether in vivo phosphorylation of IRF-3 and IRF-7 occurred in response to K1271 expression, an antibody directed against a phosphopeptide spanning Ser 477/479 of IRF-7 was raised as a complement to the previously generated IRF-3 Ser396 antibody (34). Using these phosphospecific an-

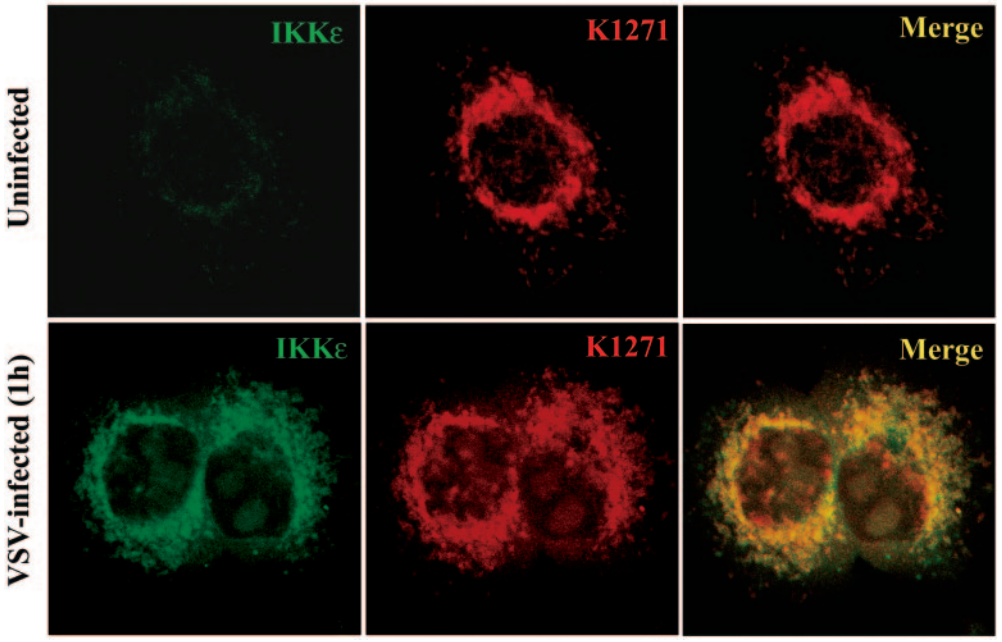

FIG. 6. Colocalization of endogenous IKKε and K1271. Human lung epithelial A549 cells, either control (upper panels) or VSV infected (lower panels), were costained for IKKε (in green) and K1271 (in red), and confocal fluorescent images were merged. IKKε was detected using mouse anti-IKKε and anti-mouse AF488 antibodies, while K1271 was detected using guinea pig anti-K1271 N-term and anti-guinea pig AF546 antibodies.

tibodies, it was possible to demonstrate that expression of ΔRIG-I, K1271, or TBK1 induced IRF-7 Ser 477/479 and IRF-3 Ser396 phosphorylation in vivo (Fig. 9B, lanes 4, 7, and 10). Coexpression of the ubiquitin-editing protein A20 (26a) or the viral NS3-4A protease completely inhibited ΔRIG-I- and K1271-induced IRF-3 and IRF-7 phosphorylation (Fig. 9B, lanes 5, 6, 8, and 9). On the other hand, TBK1-mediated phosphorylation of IRF-3 and IRF-7 was not inhibited by A20

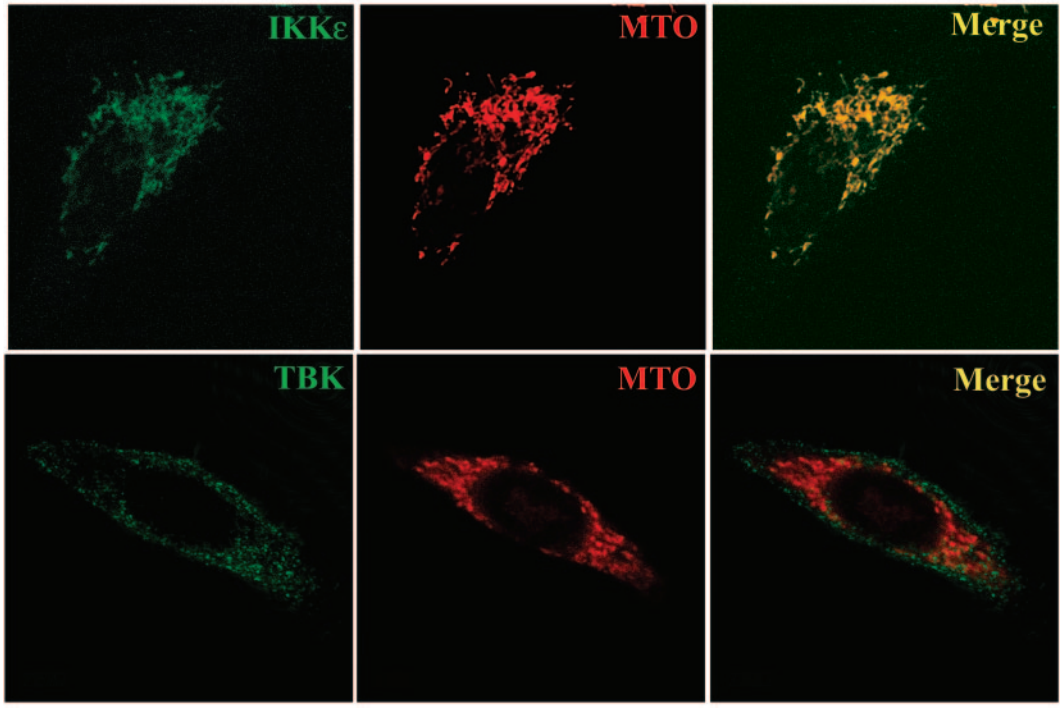

FIG. 7. Distinct subcellular localization of IKKε and TBK1. VSV-infected A549 cells were treated with MTO (in red), fixed, and stained for either IKKε (upper panels) or TBK1 (lower panels). The confocal fluorescent images were merged. IKKε was detected as described above, while TBK1 was detected using rabbit anti-TBK1 and anti-rabbit AF488 antibodies.

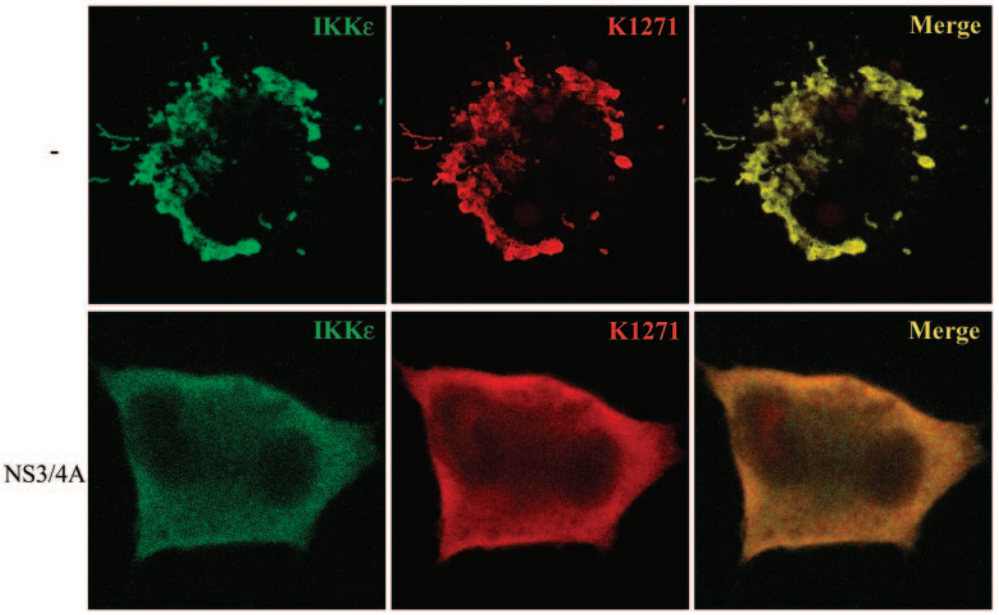

FIG. 8. Disruption of the IKKε-K1271 complex localization by expression of NS3-4A. COS-7 cells transfected with IKKε and K1271 expression plasmids, without (upper panels) or with (lower panels) a construct encoding NS3-4A, were costained for IKKε (in green) and K1271 (in red), and confocal fluorescent images were merged. IKKε and K1271 were detected as described above.

and NS3-4A, indicating that both of these inhibitory activities acted upstream of TBK1 (Fig. 9B, lanes 10 to 12) and confirming previous findings that NS3-4A has no effect on the ability of TBK-1 to phosphorylate IRF-3 (8).

K1271 activates endogenous ISG expression and the antiviral state. As a measure of the induction of the antiviral state, the constitutively active form of RIG-I, ΔRIG-I, K1271, or the TRIF adapter was used to assess the induction of endogenous IFN-stimulated gene 56 (ISG56) expression. Coexpression of ΔRIG-I, K1271, or TRIF resulted in a strong induction of endogenous ISG56 expression (Fig. 10A, lanes 5, 9, and 17). Expression of the point-mutated K1271(C508A) also induced ISG56 expression (Fig. 10A, lane 13). The cellular A20 protein completely inhibited RIG-I- and K1271-induced ISG56 expression (Fig. 10A, lanes 6, 10, and 14) but did not affect TRIF-induced ISG56 expression (Fig. 10A, lane 18). NS3-4A also totally blocked ΔRIG-I- and K1271-mediated induction of ISG56 (Fig. 10A, lanes 7 and 11); however, NS3-4A only weakly interfered with K1271(C508A)-mediated induction of ISG56 (Fig. 10A, lane 15) because NS3-4A failed to cleave K1271(C508A). In contrast, molecular weight reduction of K1271 as a result of NS3-4A cleavage was easily detected (Fig. 10A, lane 11). NS3-4A also failed to inhibit TRIF-mediated ISG56 expression. In all cases, expression of the dominant-negative form of IRF3, IRF3ΔN, inhibited ISG56 expression (Fig. 10A, lanes 8, 12, 16, and 20), demonstrating that ISG56 induction occurred through an IRF3-dependent pathway. As a further confirmation of the generation of an antiviral state, HEK293 cells expressing K1271 or IKKε were infected with VSV and the kinetics of viral protein expression was measured. Viral protein production was significantly inhibited from 6 to 9 h in control cells to 12 to 24 h in cells expressing K1271 or IKKε protein; furthermore, ISG56 expression was constitutively detected in K1271- or IKKε-expressing cells (Fig. 10B), thus demonstrating the generation of an antiviral state by K1271 that blocked VSV replication.

DISCUSSION

It has quickly become clear that the RNA helicase RIG-I pathway plays an essential role in the sensing of incoming virus infection and directly relays regulatory signals to the host antiviral response. The adapter molecule providing a link between RIG-I sensing of incoming viral RNA and downstream activation events was recently elucidated; four independent groups used high-throughput screening and/or database search analyses to identify the new signaling component, which has alternatively been termed MAVS/IPS-1-1/VISA/Cardif (20, 29, 35, 40) and is termed K1271 in this study. The fact that MAVS/IPS-1-1/VISA/Cardif localizes to the mitochondrial membrane suggests linkage among recognition of viral infection, the development of innate immunity, and mitochondrial function (35). The IKK-related kinases TBK1 and IKKε are critical downstream components of the activation of the interferon antiviral response through their ability to phosphorylate the C-terminal domains of IRF-3 and IRF-7 (13, 28, 36). In the present study, we demonstrate that VSV infection of lung epithelial A549 cells results in the induction and recruitment of IKKε to the mitochondrial membrane, in association with K1271 (MAVS/IPS-1-1/VISA/Cardif). Furthermore, the hepatitis C virus NS3-4A protease activity specifically cleaves the MAVS/IPS-1-1/VISA/Cardif-IKKε molecular complex from the mitochondria as part of its immune evasion strategy. Point mutation of Cys508 to Ala, the target residue of NS3-4A, created a MAVS/IPS-1-1/VISA/Cardif protein that not only was resistant to cleavage and subcellular relocation but also maintained the association with IKKε in the presence of protease activity. Disruption of the mitochondrial localization of

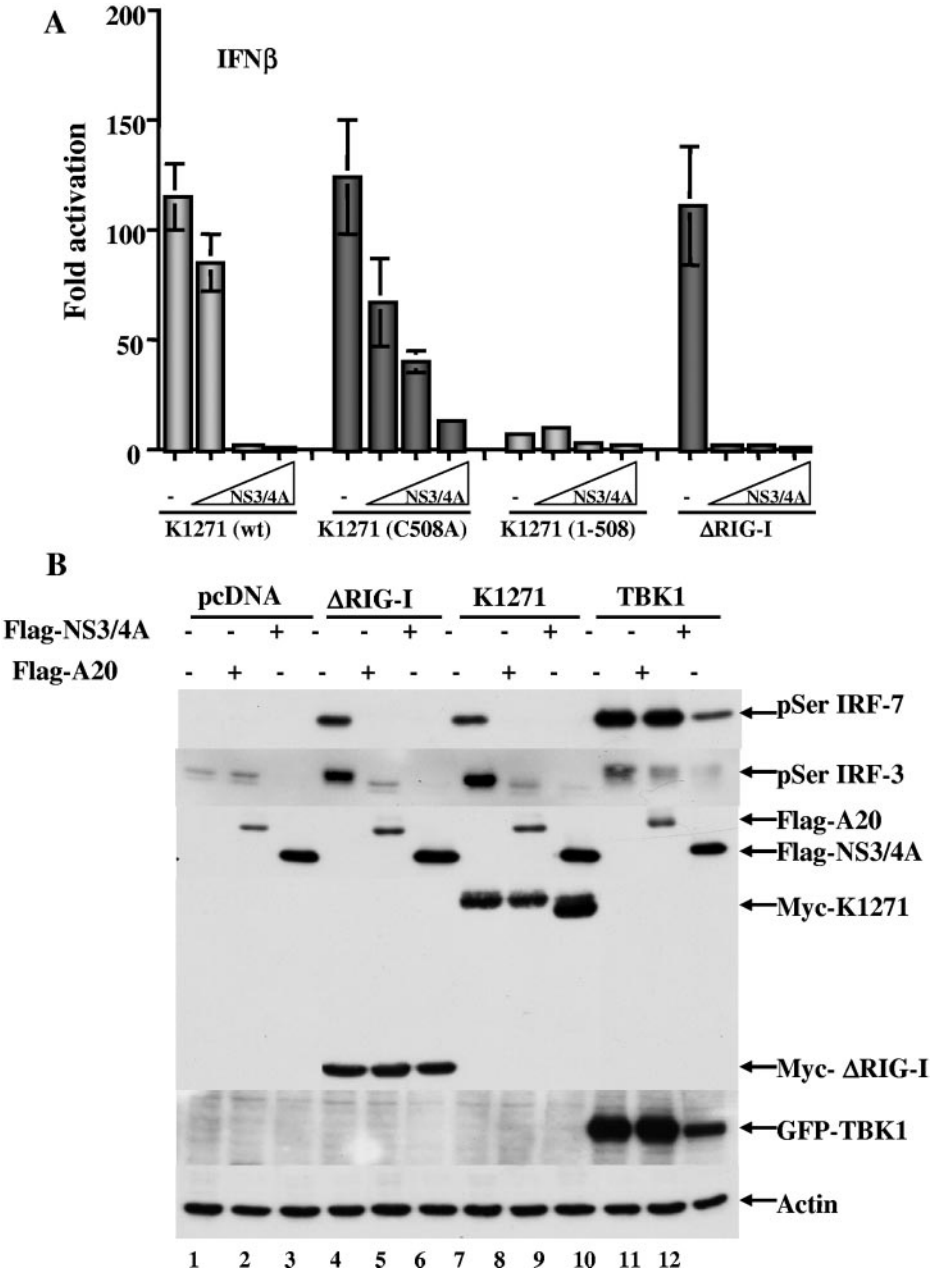

FIG. 9. Inhibition of IRF and IFN-β activation by NS3-4A. (A) Inhibition of the IFN-β promoter. HEK293 cells were transfected with 100 ng of pRLTK control plasmid, 100 ng of IFN-β–pGL3 reporter plasmid, and 200 ng of ΔRIG-I and wild-type or mutated forms of K1271 expression plasmids, together with increasing amounts of NS3-4A expression plasmid (125 ng, 500 ng, and 2,000 ng) as indicated. Luciferase activity was analyzed at 24 h posttransfection by the Dual-Luciferase reporter assay as described by the manufacturer (Promega). Relative luciferase activity was measured as activation (*n*-fold; relative to the basal level of reporter gene in the presence of pcDNA3 vector after normalization with cotransfected renilla luciferase activity); values are means ± standard deviations from three experiments. (B) A20 and NS3-4A inhibit K1271- and ΔRIG-I-mediated activation of IRF-3 and IRF-7. HEK293 cells were cotransfected with 1 μg of IRF-7, IRF-3, Myc-ΔRIG-I, Myc-K1271, or GFP-TBK1 and 2 μg of Flag-A20 or Flag–NS3-4A expression construct as indicated. Whole-cell extracts (50 μg) were resolved by sodium dodecyl sulfate-polyacrylamide gel electrophoresis and analyzed by immunoblotting for IRF-7 pSer477/479, IRF-3 pSer396, Flag-A20, Flag–NS3-4A, Myc-ΔRIG-I, Myc-K1271, GFP-TBK1, and actin.

MAVS/IPS-1-1/VISA/Cardif-IKKε also ablated downstream signaling to the IFN antiviral response. These observations provide the outline of the mechanism by which HCV evades the IFN antiviral response.

The strong and apparently selective recruitment of IKKε to the mitochondria in association with MAVS/IPS-1-1/VISA/Cardif is enigmatic, given that TBK1 is involved principally in downstream signaling to IRF-3 and IRF-7 phosphorylation and development of the antiviral response (13, 28, 36). Studies of TBK1 and IKKε knockout mice demonstrate a clear role for TBK1 in the generation of the antiviral response, with an accessory role associated to date with IKKε (17, 31). Given that

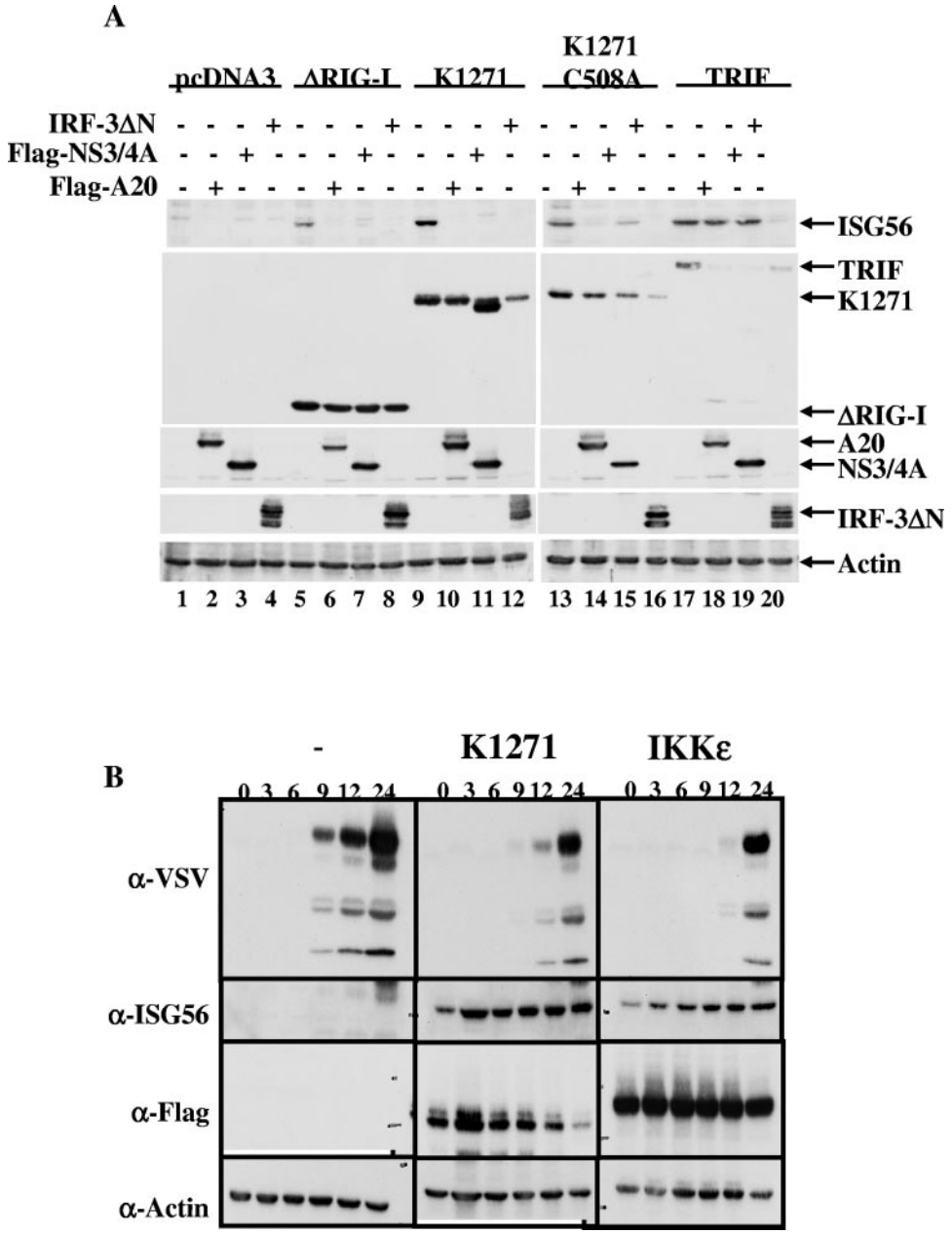

FIG. 10. (A) NS3-4A and A20 inhibit K1271-mediated activation of endogenous ISG56 gene expression. HEK293 cells were cotransfected with 1 μg of pcDNA3, Myc-ΔRIG-I, Myc-KIAA1271, Myc-KIAA1271(C508A), or Myc-TRIF and 2 μg of IRF-3ΔN, Flag-A20, or Flag–NS3-4A expression construct as indicated. Whole-cell extracts (50 μg) were resolved by sodium dodecyl sulfate-polyacrylamide gel electrophoresis and analyzed by immunoblotting using antibodies to ISG56, Myc, Flag, IRF-3, and actin. (B) K1271 inhibits VSV replication. HEK293 cell lines expressing K1271 or IKKε were infected with VSV (1 multiplicity of infection), and viral protein expression was measured at different times after infection by immunoblotting. Expression of the Flag-tagged transgene and the endogenous ISG56 was also monitored.

IKKε knockout mice do not appear to have major defects in IFN induction, the targeting of an IKKε-dependent pathway does not explain the inhibition of IFN induction by the hepatitis C protease. Selective recruitment of IKKε may reflect a distinct functional role for this kinase activity in the host response to virus infection, perhaps at the level of coordinating mitochondrion-dependent cell death in virus-infected cells. Ongoing biochemical studies have demonstrated that a small proportion of total TBK1 is present in highly purified mitochondrial fractions (Q. Sun, unpublished data); whether this fraction is enzymatically active and/or physically associated with MAVS/IPS-1-1/VISA/Cardif remains to be determined. Although colocalization of TBK1 with the mitochondria and MAVS/IPS-1-1/VISA/Cardif may be transient and may not be easily detected by confocal analysis, the observation that IKKε is so intimately associated with MAVS/IPS-1-1/VISA/Cardif is not easily resolved at this point. However, in support of a functional role of IKKε in HCV pathogenesis, previous ex-

periments have demonstrated that IKKε overexpression, but not the expression of TBK1 or other signaling adapters, partially reversed HCV protease-mediated inhibition of IFN induction (8).

The mechanism of recruitment of IKKε to the mitochondria remains unclear at present. However, given that NS3-4A is still able to block IFN-β promoter activity when the Cys508-to-Ala point-mutated MAVS/IPS-1-1/VISA/Cardif protein is expressed, albeit with a 10-fold-reduced efficiency, it is possible that another adapter downstream of MAVS/IPS-1-1/VISA/Cardif may be targeted by NS3-4A. Alternatively, an additional mechanism involved in the recruitment of IKKε to the MAVS/IPS-1-1/VISA/Cardif mitochondrial reticulotubular network may be affected by the HCV protease. We have also identified significant changes in mitochondrial reticulotubular architecture following VSV infection and the recruitment of IKKε to the mitochondria, suggesting that IKKε may be contributing to virus-induced apoptosis.

Seth et al. identified the localization of MAVS to the mitochondrial membrane and also showed that MAVS moved into a detergent-resistant mitochondrial fraction upon viral infection (35). The fact that MAVS functionality requires mitochondrial association suggests linkage among recognition of viral infection, the development of innate immunity, and virus-induced mitochondrion-dependent cell death. In fact, knockdown of *MAVS* gene expression by small interfering RNAs increased apoptosis, possibly hinting at a protective role for MAVS during the early stages of viral infection. Potentially, the activation of other components of the mitochondrial membrane could also contribute to signaling to the antiviral response. In support of this idea, MAVS colocalizes in the same detergent-insoluble fraction as the antiapoptotic protein Bcl-xL. Among the many CARD-containing proteins with roles in apoptosis and immunity (Apaf1, NOD1, NOD2 RIP2, and RIG-I), MAVS is unique (7, 11, 12). The localization of this CARD domain-containing adapter to the mitochondrial membrane is highly strategic and may help the host cell to sense incoming viral challenge and coordinate an immune or apoptotic response, depending on the pathogen. Many viruses replicate in intracellular organelles, such as the endoplasmic reticulum; a good example is HCV, which replicates in the membranous web that connects the endoplasmic reticulum to the mitochondria. dsRNA structures, possibly within replicating ribonucleoprotein complexes, may be recognized by RIG-I and/or Mda-5, resulting in downstream signaling through MAVS. Mitochondria may be at the center of a delicate balancing act between the host immune response and virus-induced apoptosis. In the case of HCV infection, cleavage of MAVS by the NS3-4A protease appears to tip the balance, resulting in disruption of innate immune responses and the establishment of chronic HCV persistence (15).

The identification of MAVS/IPS-1/VISA/Cardif and its role in innate signaling and its characterization as the physiologically relevant target of the NS3-4A protease are important steps in the complete understanding of the mechanisms by which HCV evades the early host response. The essential localization of this CARD domain-containing adapter to the mitochondria furthermore suggests an important function in the coordination of the innate immune and apoptotic responses. The implications for the study of HCV pathogenesis are particularly profound, given that experimental compounds, such as BILN2061 and VX-950, that block NS3-4A protease activity may accomplish two goals: inhibition of virus multiplication and processing and restoration of the early innate immune response that is critical to the development of a robust adaptive response in patients (9, 22).

ACKNOWLEDGMENTS

We thank Hong-Bing Shu, Zhijian Chen, Ganes Sen, Wen-Zhe Ho, and Michael Gale for reagents used in this study and members of the Molecular Oncology Group, Lady Davis Institute, for helpful discussions.

This research was supported by grants from the Canadian Institutes of Health Research (J.H. and R.L.), CANVAC, and the Canadian Network for Vaccines and Immunotherapeutics (J.H.) and by the National Cancer Institute of Canada, with the support of the Canadian Cancer Society (J.H.). D.V. was supported by l'Agence Nationale de la Recherche sur le Sida (ANRS). R.L. was supported by an FRSQ Chercheur-boursier and J.H. by a CIHR Senior Investigator award.

REFERENCES

1. **Akira, S., and K. Takeda.** 2004. Toll-like receptor signalling. Nat. Rev. Immunol. **4:**499–511.
2. **Alexopoulou, L., A. C. Holt, R. Medzhitov, and R. A. Flavell.** 2001. Recognition of double-stranded RNA and activation of NF-kappaB by Toll-like receptor 3. Nature **413:**732–738.
3. **Alter, H. J., and L. B. Seeff.** 2000. Recovery, persistence, and sequelae in hepatitis C virus infection: a perspective on long-term outcome. Semin. Liver Dis. **20:**17–35.
4. **Andrejeva, J., K. S. Childs, D. F. Young, T. S. Carlos, N. Stock, S. Goodbourn, and R. E. Randall.** 2004. The V proteins of paramyxoviruses bind the IFN-inducible RNA helicase, mda-5, and inhibit its activation of the IFN-beta promoter. Proc. Natl. Acad. Sci. USA **101:**17264–17269.
5. **Blight, K. J., A. A. Kolykhalov, and C. M. Rice.** 2000. Efficient initiation of HCV RNA replication in cell culture. Science **290:**1972–1974.
6. **Blight, K. J., J. A. McKeating, J. Marcotrigiano, and C. M. Rice.** 2003. Efficient replication of hepatitis C virus genotype 1a RNAs in cell culture. J. Virol. **77:**3181–3190.
7. **Bouchier-Hayes, L., and S. J. Martin.** 2002. CARD games in apoptosis and immunity. EMBO Rep. **3:**616–621.
8. **Breiman, A., N. Grandvaux, R. Lin, C. Ottone, S. Akira, M. Yoneyama, T. Fujita, J. Hiscott, and E. F. Meurs.** 2005. Inhibition of RIG-I-dependent signaling to the interferon pathway during hepatitis C virus expression and restoration of signaling by IKKε. J. Virol. **79:**3969–3978.
9. **Chen, S. H., and S. L. Tan.** 2005. Discovery of small-molecule inhibitors of HCV NS3-4A protease as potential therapeutic agents against HCV infection. Curr. Med. Chem. **12:**2317–2342.
10. **Choo, Q. L., G. Kuo, A. J. Weiner, L. R. Overby, D. W. Bradley, and M. Houghton.** 1989. Isolation of a cDNA clone derived from a blood-borne non-A, non-B viral hepatitis genome. Science **244:**359–362.
11. **Damiano, J. S., R. M. Newman, and J. C. Reed.** 2004. Multiple roles of CLAN (caspase-associated recruitment domain, leucine-rich repeat, and NAIP CIIA HET-E, and TP1-containing protein) in the mammalian innate immune response. J. Immunol. **173:**6338–6345.
12. **Damiano, J. S., and J. C. Reed.** 2004. CARD proteins as therapeutic targets in cancer. Curr. Drug Targets **5:**367–374.
13. **Fitzgerald, K. A., S. M. McWhirter, K. L. Faia, D. C. Rowe, E. Latz, D. T. Golenbock, A. J. Coyle, S. M. Liao, and T. Maniatis.** 2003. IKKepsilon and TBK1 are essential components of the IRF3 signaling pathway. Nat. Immunol. **4:**491–496.
14. **Foy, E., K. Li, R. Sumpter, Jr., Y. M. Loo, C. L. Johnson, C. Wang, P. M. Fish, M. Yoneyama, T. Fujita, S. M. Lemon, and M. Gale, Jr.** 2005. Control of antiviral defenses through hepatitis C virus disruption of retinoic acid-inducible gene-I signaling. Proc. Natl. Acad. Sci. USA **102:**2986–2991.
15. **Gale, M., Jr., and E. M. Foy.** 2005. Evasion of intracellular host defence by hepatitis C virus. Nature **436:**939–945.
16. **He, Y., and M. G. Katze.** 2002. To interfere and to anti-interfere: the interplay between hepatitis C virus and interferon. Viral Immunol. **15:**95–119.
17. **Hemmi, H., O. Takeuchi, S. Sato, M. Yamamoto, T. Kaisho, H. Sanjo, T. Kawai, K. Hoshino, K. Takeda, and S. Akira.** 2004. The roles of two IkappaB kinase-related kinases in lipopolysaccharide and double stranded RNA signaling and viral infection. J. Exp. Med. **199:**1641–1650.
18. **Kang, D. C., R. V. Gopalkrishnan, Q. Wu, E. Jankowsky, A. M. Pyle, and P. B. Fisher.** 2002. mda-5: an interferon-inducible putative RNA helicase with double-stranded RNA-dependent ATPase activity and melanoma growth-suppressive properties. Proc. Natl. Acad. Sci. USA **99:**637–642.

19. **Kato, H., S. Sato, M. Yoneyama, M. Yamamoto, S. Uematsu, K. Matsui, T. Tsujimura, K. Takeda, T. Fujita, O. Takeuchi, and S. Akira.** 2005. Cell type-specific involvement of RIG-I in antiviral response. Immunity **23:**19–28.
20. **Kawai, T., K. Takahashi, S. Sato, C. Coban, H. Kumar, H. Kato, K. J. Ishii, O. Takeuchi, and S. Akira.** 2005. IPS-1, an adaptor triggering RIG-I- and Mda5-mediated type I interferon induction. Nat. Immunol. **6:**981–988.
21. **Kiyosawa, K., T. Sodeyama, E. Tanaka, Y. Gibo, K. Yoshizawa, Y. Nakano, S. Furuta, Y. Akahane, K. Nishioka, R. H. Purcell, et al.** 1990. Interrelationship of blood transfusion, non-A, non-B hepatitis and hepatocellular carcinoma: analysis by detection of antibody to hepatitis C virus. Hepatology **12:**671–675.
22. **Lamarre, D., P. C. Anderson, M. Bailey, P. Beaulieu, G. Bolger, P. Bonneau, M. Bos, D. R. Cameron, M. Cartier, M. G. Cordingley, A. M. Faucher, N. Goudreau, S. H. Kawai, G. Kukolj, L. Lagace, S. R. LaPlante, H. Narjes, M. A. Poupart, J. Rancourt, R. E. Sentjens, R. St. George, B. Simoneau, G. Steinmann, D. Thibeault, Y. S. Tsantrizos, S. M. Weldon, C. L. Yong, and M. Llinas-Brunet.** 2003. An NS3 protease inhibitor with antiviral effects in humans infected with hepatitis C virus. Nature **426:**186–189.
22a. **Li, K., E. Foy, J. C. Ferreon, M. Nakamura, A. C. Ferreon, M. Ikeda, S. C. Ray, M. Gale, Jr., and S. M. Lemon.** 2005. Immune evasion by hepatitis C virus NS3/4A protease-mediated cleavage of the Toll-like receptor 3 adaptor protein TRIF. Proc. Natl. Acad. Sci. USA **102:**2992–2997.
23. **Li, X. D., L. Sun, R. B. Seth, G. Pineda, and Z. J. Chen.** 2005. Hepatitis C virus protease NS3/4A cleaves mitochondrial antiviral signaling protein off the mitochondria to evade innate immunity. Proc. Natl. Acad. Sci. USA **102:**17717–17722.
24. **Lin, R., P. Beauparlant, C. Makris, S. Meloche, and J. Hiscott.** 1996. Phosphorylation of IκBα in the C-terminal PEST domain by casein kinase II affects intrinsic protein stability. Mol. Cell. Biol. **16:**1401–1409.
25. **Lin, R., P. Génin, Y. Mamane, and J. Hiscott.** 2000. Selective DNA binding and association with the CREB binding protein coactivator contribute to differential activation of alpha/beta interferon genes by interferon regulatory factors 3 and 7. Mol. Cell. Biol. **20:**6342–6353.
26. **Lin, R., C. Heylbroeck, P. M. Pitha, and J. Hiscott.** 1998. Virus-dependent phosphorylation of the IRF-3 transcription factor regulates nuclear translocation, transactivation potential, and proteasome-mediated degradation. Mol. Cell. Biol. **18:**2986–2996.
26a. **Lin, R., L. Yang, P. Nakhaei, Q. Sun, E. Sharif-Askari, I. Julkunen, and J. Hiscott.** 2006. Negative regulation of the retinoic acid-inducible gene I-induced antiviral state by the ubiquitin-editing protein A20. J. Biol. Chem. **281:**2095–2103.
27. **Maniatis, T., J. V. Falvo, T. H. Kim, T. K. Kim, C. H. Lin, B. S. Parekh, and M. G. Wathelet.** 1998. Structure and function of the interferon-beta enhanceosome. Cold Spring Harbor Symp. Quant. Biol. **63:**609–620.
28. **McWhirter, S. M., K. A. Fitzgerald, J. Rosains, D. C. Rowe, D. T. Golenbock, and T. Maniatis.** 2004. IFN-regulatory factor 3-dependent gene expression is defective in Tbk1-deficient mouse embryonic fibroblasts. Proc. Natl. Acad. Sci. USA **101:**233–238.
29. **Meylan, E., J. Curran, K. Hofmann, D. Moradpour, M. Binder, R. Bartenschlager, and J. Tschopp.** 2005. Cardif is an adaptor protein in the RIG-I antiviral pathway and is targeted by hepatitis C virus. Nature **437:**1167–1172.
30. **Munshi, N., J. Yie, M. Merika, K. Senger, S. Lomvardas, T. Agalioti, and D. Thanos.** 1999. The IFN-beta enhancer: a paradigm for understanding activation and repression of inducible gene expression. Cold Spring Harbor Symp. Quant. Biol. **64:**149–159.
31. **Perry, A. K., E. K. Chow, J. B. Goodnough, W. C. Yeh, and G. Cheng.** 2004. Differential requirement for TANK-binding kinase-1 in type I interferon responses to Toll-like receptor activation and viral infection. J. Exp. Med. **199:**1651–1658.
32. **Rehermann, B., and M. Nascimbeni.** 2005. Immunology of hepatitis B virus and hepatitis C virus infection. Nat. Rev. Immunol. **5:**215–229.
33. **Rosenberg, S.** 2001. Recent advances in the molecular biology of hepatitis C virus. J. Mol. Biol. **313:**451–464.
34. **Servant, M. J., N. Grandvaux, B. R. tenOever, D. Duguay, R. Lin, and J. Hiscott.** 2003. Identification of the minimal phosphoacceptor site required for in vivo activation of interferon regulatory factor 3 in response to virus and double-stranded RNA. J. Biol. Chem. **278:**9441–9447.
35. **Seth, R. B., L. Sun, C. K. Ea, and Z. J. Chen.** 2005. Identification and characterization of MAVS, a mitochondrial antiviral signaling protein that activates NF-kappaB and IRF 3. Cell **122:**669–682.
36. **Sharma, S., B. R. tenOever, N. Grandvaux, G. P. Zhou, R. Lin, and J. Hiscott.** 2003. Triggering the interferon antiviral response through an IKK-related pathway. Science **300:**1148–1151.
37. **Sumpter, R., Jr., Y. M. Loo, E. Foy, K. Li, M. Yoneyama, T. Fujita, S. M. Lemon, and M. Gale, Jr.** 2005. Regulating intracellular antiviral defense and permissiveness to hepatitis C virus RNA replication through a cellular RNA helicase, RIG-I. J. Virol. **79:**2689–2699.
38. **Wasley, A., and M. J. Alter.** 2000. Epidemiology of hepatitis C: geographic differences and temporal trends. Semin. Liver Dis. **20:**1–16.
39. **Wieland, S. F., and F. V. Chisari.** 2005. Stealth and cunning: hepatitis B and hepatitis C viruses. J. Virol. **79:**9369–9380.
40. **Xu, L. G., Y. Y. Wang, K. J. Han, L. Y. Li, Z. Zhai, and H. B. Shu.** 2005. VISA is an adapter protein required for virus-triggered IFN-beta signaling. Mol. Cell **19:**727–740.
41. **Yoneyama, M., M. Kikuchi, T. Natsukawa, N. Shinobu, T. Imaizumi, M. Miyagishi, K. Taira, S. Akira, and T. Fujita.** 2004. The RNA helicase RIG-I has an essential function in double-stranded RNA-induced innate antiviral responses. Nat. Immunol. **5:**730–737.